Multilevel Signaling for Increasing the Reach of 10 Gb/s Lightwave Systems

Sheldon Walklin, *Member, IEEE*, and Jan Conradi, *Senior Member, IEEE*

***Abstract*—Polybinary, optical amplitude modulated phase shift keying (AM-PSK) polybinary, M-ary amplitude shift keying (ASK), and polyquaternary signaling schemes operating at 10 Gb/s are investigated in 1550-nm lightwave systems operating over standard, single-mode fiber. The premise for exploring these signal types is that they concentrate power at frequencies closer to the optical carrier where phase distortion of the optical field from chromatic dispersion is less severe. Issues such as modulator chirp, optimal level spacing in a 4-ary ASK signal, and phase modulated to amplitude modulated (PM–AM) noise conversion from a nonzero laser linewidth are studied. It is found that higher order polybinary signals do not offer an improvement in dispersion tolerance over a duobinary signal. 4-ary ASK is demonstrated to increase the dispersion-limited distance to 225 km experimentally and 350 km through simulation, but at the expense of a $\sim$8 dB degradation in receiver sensitivity due to the increased number of levels and the signal dependence of signal-spontaneous beat noise. Furthermore, the linewidth requirement for a 4-ary ASK signal is less than 1 MHz in order to minimize the impact of PM–AM relative intensity noise (RIN) when transmitting over 200–300 km.**

***Index Terms*—Bandwidth compression, optical fiber communication, optical modulation/demodulation, optical propagation in dispersive media.**

I. Introduction

SINCE the advent of erbium-doped fiber amplifiers (EDFA's), attention has shifted away from considerations of available power at the receiver to limitations due to chromatic dispersion in lightwave systems operating at $\sim$1550 nm over standard, single-mode fiber. It is well known that bandwidth and power can be traded off for one another and it is, therefore, of interest to investigate various forms of multilevel signaling for their potential dispersion tolerance. It has already been demonstrated that multilevel signaling can extend the reach of 10 Gb/s lightwave systems beyond the $\sim$100 km possible in a conventional binary system. For example, in [1] a duobinary filter was used at the receiver to generate a three-level electrical duobinary signal from a received binary, intensity-modulated signal to realize an improved dispersion tolerance. Transmission of a duobinary, intensity-modulated signal (three optical intensity levels) was experimentally demonstrated in [2], [3] to extend the dispersion-limited distance. Yet another duobinary signaling scheme, now receiving much attention, uses a combination of amplitude modulation and phase-shift keying of the optical carrier (optical AM-PSK duobinary) [4], [5] and has been demonstrated at distances up to 168 km [6] and 210 km [7]. High-capacity WDM systems have also been demonstrated recently using optical AM-PSK duobinary signaling [8], [9]. Four-level signaling, too, has been demonstrated experimentally at 10 Gb/s using 4-ary ASK for distances up to 225 km [10], and at 20 Gb/s over 46 km using dispersion supported transmission (DST) [11].

This present paper evaluates and compares the transmission performance of a variety of multilevel signaling schemes including polybinary, AM-PSK polybinary, M-ary ASK and polyquaternary. All of these signaling schemes result in a power spectral density (PSD) that is more concentrated about the optical carrier where the quadratic phase distortion of the fiber's transfer function is expected to have less impact, which is the premise for exploring them. Issues such as RIN from PM to AM noise conversion, accumulation of amplified spontaneous emission (ASE) noise, optimal level spacing in M-ary signals, and frequency chirping in external modulators are investigated. Finally, experimental results for a 10 Gb/s 4-ary ASK system, beyond those presented in [10], are given here and compared to results from realistic simulations.

This paper summarizes much of the work in [24].

II. Multilevel Signaling Schemes

A description of the various multilevel signals explored is given below.

A. Polybinary Signals

Polybinary signals are a class of partial-response signals that were first described by Lender [12], [13]. A polybinary signal is generated by introducing correlation among adjacent bits in a binary signal and has the interesting attribute that the PSD is redistributed such that it is more concentrated about the optical carrier. A polybinary signal can be obtained by passing a binary signal through the delay-and-add filter shown in Fig. 1. Assuming there are $b-2$ delay elements, a multilevel signal with b levels results at the output of a polybinary filter, with a PSD that is compressed by a factor $b-1$ compared to a binary signal. Assuming the input binary sequence is made up of ideal NRZ pulses with height A and period T, the PSD of a polybinary signal is given by [12]

$$S(f) = \frac{(b-1)^2 A^2 T}{4} \operatorname{sinc}^2[(b-1)fT]. \quad (1)$$

Manuscript received January 15, 1999; revised July 9, 1999. This work was supported by the Natural Sciences and Engineering Research Council (NSERC) of Canada, Nortel and TRLabs through the NSERC/Nortel/TRLabs Industrial Research Chair in Fiber Optic Communications at the University of Alberta, Canada.

The authors are with the Telecommunications Research Laboratories—TR Labs., Edmonton, Alta. T5K 2P7 Canada.

Publisher Item Identifier S 0733-8724(99)08005-6.

0733–8724/99$10.00 © 1999 IEEE

A. Soto and W. Soto
Authorized licensed use limited to: University of Nevada Las Vegas. Downloaded on June 10,2023 at 20:47:21 UTC from IEEE Xplore. Restrictions apply. IPR2023-00838
Exhibit 2002
Page 1

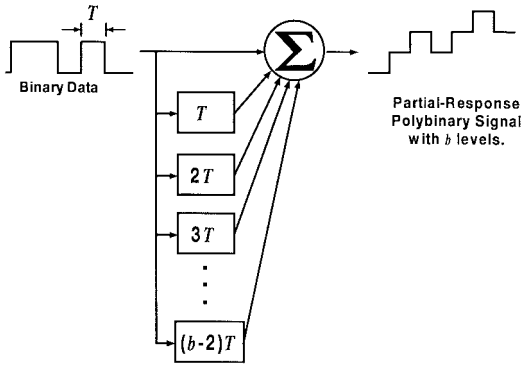


Fig. 1. Filter for generating a polybinary signal.

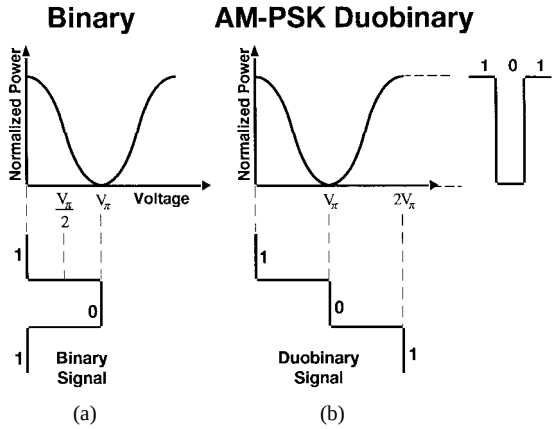


Fig. 2. (a) MZ bias and drive condition for generating a conventional binary, intensity-modulated signal and (b) an optical AM-PSK duobinary signal.

Note that, regardless of the number of levels in a polybinary signal, each polybinary symbol carries one bit of information, only. Provided the original data sequence $\{a_k\}$ is first precoded into the binary sequence $\{b_k\}$ according to

$$b_k = a_k \oplus b_{k-1} \oplus b_{k-2} \cdots \oplus b_{k-(b-2)} \tag{2}$$

prior to being input to the polybinary filter of Fig. 1 to generate the polybinary signal

$$c_k = b_k + b_{k-1} + \cdots + b_{k-(b-2)} \tag{3}$$

the original binary sequence can be recovered from independent decisions on $\{c_k\}$, through

$$a_k = c_k \bmod 2. \tag{4}$$

Note that a duobinary signal is a polybinary signal with $b = 3$, i.e., the polybinary filter contains one delay element.

B. AM-PSK Polybinary Signals

With these signals, the multiple levels are encoded in both the amplitude and phase of the carrier [12], [13]. For lightwave systems, an AM-PSK polybinary signal can be generated by applying a baseband, electrical polybinary signal to a Mach–Zehnder (MZ) external modulator biased at maximum extinction [4], [5], as shown in Fig. 2 for the case $b = 3$. The phase shift keying of the carrier occurs each time the applied electrical signal passes through the point of maximum extinction in the MZ's transfer characteristic. When a duobinary electrical signal is applied to the modulator, a binary intensity-modulated signal results that can be decoded by a conventional discriminator. Hence, there is no inherent degradation in the receiver's sensitivity compared to a conventional binary signal. However, the PSD of the optical field about the carrier is that of a duobinary signal, which can be transmitted in a bandwidth of $\pm B/2$ about the optical carrier where B is the bit rate. This bandwidth requirement is one-half that of a conventional binary signal. In general, if a polybinary signal with b levels (where b is odd) is applied to an MZ biased as in Fig. 2, an AM-PSK polybinary signal results with $(b+1)/2$ intensity levels where decisions on the individual symbols in the intensity-modulated signal are sufficient to decode the binary information.

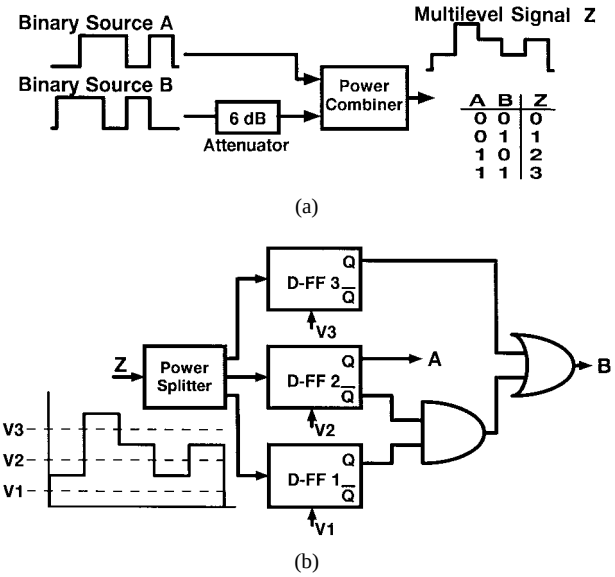


Fig. 3. (a) Multilevel symbol generator and (b) multilevel decoder.

C. M-ary ASK and Polyquaternary Signals

An M-ary ASK optical intensity signal can be obtained by applying an M-ary electrical signal to an MZ biased at the half power point of its transfer characteristic. Generating a 4-ary electrical signal from two binary tributaries at Gb/s rates can be accomplished using the circuit shown in Fig. 3(a). At the receiver, direct detection can be used to convert the 4-ary intensity-modulated optical signal back to a 4-ary electrical signal, and the binary tributaries can then be recovered using the decoder circuit shown in Fig. 3(b), which uses three independent decision circuits.

The transmission bandwidth of an M-ary signal is scaled by a factor $1/\log_2(M)$ compared to a binary signal operating at the same bit rate, where M is the number of levels in the M-ary signal. Similarly, the symbol period is increased by a factor $\log_2(M)$ compared to a binary signal. This is unlike a polybinary signal, in which the symbol period is the same, regardless of the number of levels.

It is also possible to introduce correlation among adjacent multilevel symbols in an M-ary signal by passing the M-ary signal through the same filter as in Fig. 1. When there is one delay element in the filter of Fig. 1, a 4-ary signal at the input will produce a polyquaternary signal at the output with

A. Soto and W. Soto
Authorized licensed use limited to: University of Nevada Las Vegas. Downloaded on June 10,2023 at 20:47:21 UTC from IEEE Xplore. Restrictions apply. IPR2023-00838
Exhibit 2002
Page 2

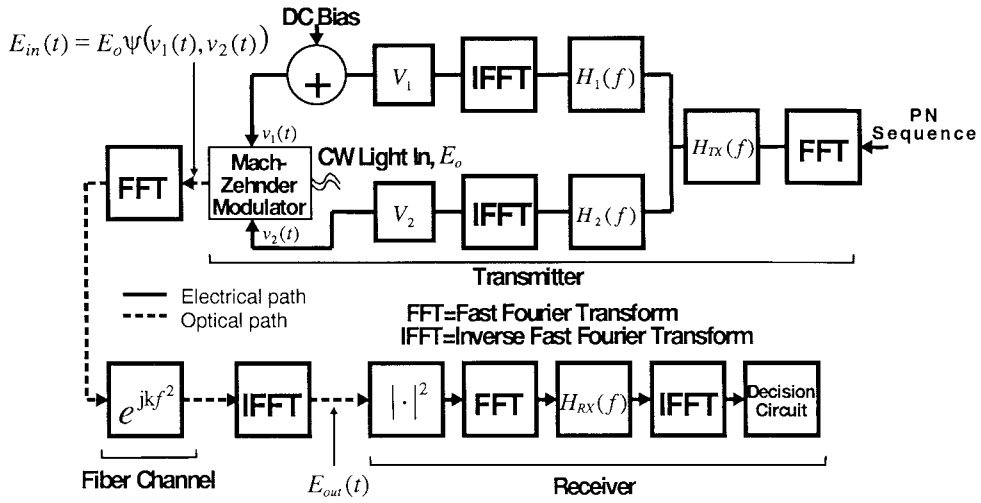


Fig. 4. Block diagram of model for computing system response: $H_{TX}(f)$ = transfer function operating on overall transmitter electrical signal; $H_1(f)$ and $H_2(f)$ are transfer functions to account for additional filtering in each arm of the modulator; ψ = MZ electrical field-domain transfer characteristic; V_1 and V_2 are scaling factors (may be negative); $E_{\rm in}(t)$ = lowpass-equivalent optical field at input; $E_{\rm out}(t)$ = lowpass-equivalent optical field at output; $H_{RX}(f)$ = transfer function for overall electrical receiver frequency response.

seven levels. Letting $\{a_k\}$ now be the input 4-ary sequence, $\{b_k\}$ a precoded 4-ary sequence, and $\{c_k\}$ the seven-level polyquaternary sequence, it is possible to recover the original 4-ary sequence from independent decisions on $\{c_k\}$, provided the following relationships are used [14]:

$$\begin{aligned} b_k &= a_k - b_{k-1} \bmod 4 \\ c_k &= b_k + b_{k-1} \\ a_k &= c_k \bmod 4. \end{aligned} \tag{5}$$

III. System Modeling

A. Model for System Response

The electrical transmitter and receiver are modeled as linear baseband systems, and nonlinear time-domain transformations are used at the transmitter and receiver to map between the electrical baseband signal and the low-pass equivalent optical signal. The fiber is modeled using a low-pass equivalent representation of a linear bandpass system in which the fiber dispersion is accounted for through the quadratic (nonlinear) phase response of the fiber's transfer function, given by

$$H_{\rm fib}(f) = \exp\left(j\frac{\pi D L \lambda^2 f^2}{c}\right) \tag{6}$$

where c is the free-space speed of light, λ is the operating wavelength, L is the fiber length, and $D \approx 17$ ps/(km·nm) is the fiber's linear dispersion coefficient. Fig. 4 shows a block diagram of the model used in calculating the system's response.

For simulations using a $LiNbO_3$ external modulator, the optical field at the output of the MZ is given by $E_o\psi(t)$ where E_o is the amplitude of a continuous-wave source input to the MZ, and $\psi(t)$ is the MZ's transfer characteristic, given by

$$\psi(v_1(t), v_2(t)) = \frac{1}{2}\exp\left(j\frac{\pi v_1(t)}{V_\pi}\right) + \frac{\gamma}{2}\exp\left(j\frac{\pi v_2(t)}{V_\pi}\right) \tag{7}$$

where V_π is the MZ's switching voltage, $v_1(t)$ and $v_2(t)$ are the voltages applied to the electrodes associated with each arm of the MZ, and the parameter γ accounts for asymmetry in the input and/or output Y-branches, and/or an unequal loss through the MZ arms. The parameter γ is always in the range $0 \le \gamma \le 1$ and relates directly to the intrinsic optical extinction ratio of the MZ, through

$$\gamma = \frac{\sqrt{\delta}-1}{\sqrt{\delta}+1} \tag{8}$$

where δ is the ratio of maximum power to minimum power measured at the output of the MZ under static (dc) conditions. For a real device, which will always have a finite extinction ratio, residual chirp will always be present [15].

B. Noise Modeling, BER, and Receiver Sensitivity Calculations

A noise model based on the theory in [16] was used in all simulations, which assume the use of an optical preamplifier. In [16, eq. (49)] the noise current can be simplified and expressed in terms of a single index n that indexes each sample in a discrete-time representation. Assuming an EDFA preamp with gain G, input coupling efficiency η_i and output coupling efficiency η_o, the noise current at time τ can be expressed as

$$\begin{aligned} \langle i^2(\tau)\rangle =& \Re\, q\eta_i G\eta_o \sum_n P(n\Delta t)h^2(\tau - n\Delta t)\Delta t \\ &+ qI_{\rm dark}\sum_n h^2(n\Delta t)\Delta t \\ &+ P_{\rm ASE}\,\Re\, q\eta_o \sum_n h^2(\tau - n\Delta t)\Delta t \\ &+ \frac{(P_{\rm ASE}\,\Re\,\eta_o)^2}{B_o}\sum_n h^2(\tau - n\Delta t)\Delta t \\ &+ \frac{2P_{\rm ASE}\,\Re^2\,\eta_i G\eta_o^2}{B_o}\sum_n P(n\Delta t)h^2(\tau - n\Delta t)\Delta t \\ &+ \frac{2kT_eF}{R_e}\sum_n h^2(n\Delta t) \\ &+ \frac{{\rm RIN}(\eta_i G\eta_o\,\Re)^2}{2B_e}\sum_n P^2(n\Delta t)h^2(\tau - n\Delta t)\Delta t \end{aligned} \tag{9}$$

A. Soto and W. Soto
Authorized licensed use limited to: University of Nevada Las Vegas. Downloaded on June 10,2023 at 20:47:21 UTC from IEEE Xplore. Restrictions apply. IPR2023-00838
Exhibit 2002
Page 3

where $\Re$ is the photodiode responsivity, q is the charge of an electron, $P(t)$ is the received optical power, $h(t)$ is the impulse response of the receiver, Δt is the simulation sampling interval, $I_{\rm dark}$ is the photodiode dark current, $P_{\rm ASE} = 2h\upsilon N_{\rm sp}(G-1)B_o$ is the ASE in an optical bandwidth B_o where $h\upsilon$ is the photon energy and $N_{\rm sp}$ is the spontaneous emission factor of the EDFA, and k is Boltzmann's constant. T_e, F, R_e, and B_e are, respectively, the temperature in Kelvins, noise factor, thermal noise resistance, and noise-equivalent bandwidth (NEB) of the electrical receiver. RIN in (9) is the total RIN falling within the bandwidth of the receiver; hence, RIN/B_e can be interpreted as an average RIN spectral density. The noise terms in (9) can be identified, respectively, as signal shot noise, dark current shot noise, shot noise from ASE, spontaneous-spontaneous beat noise, signal-spontaneous beat noise, receiver thermal noise, and RIN. The last two noise terms are in addition to those accounted for in [16].

In [16], a constraint imposed is that the simulation sampling interval Δt and the bandwidth of the optical filter following the EDFA preamp are related by $B_o = 1/\Delta t$. Hence, to avoid spectral aliasing in a simulation, B_o would have to be set large compared to the symbol rate. This constraint does not seem necessary, however, when expressing the total noise current in the form of (9) where terms $1/\Delta t$ have been replaced by B_o. If the summations in (9) are then interpreted as discrete-time approximations to integrations, the following continuous-time expressions are suggested for the signal-dependent noise terms:

$$\begin{aligned}\langle i^2(\tau)\rangle_{\rm sig} &= q\,\Re\,\eta_i G\eta_o \int P(t)h^2(\tau-t)\,dt\\ \langle i^2(\tau)\rangle_{\rm sig\text{-}sp} &= \frac{2P_{\rm ASE}\eta_i G\eta_o^2\,\Re^2}{B_o}\int P(t)h^2(\tau-t)\,dt\\ \langle i^2(\tau)\rangle_{\rm RIN} &= \frac{{\rm RIN}(\eta_i G\eta_o\,\Re)^2}{2B_e}\int P^2(t)h^2(\tau-t)\,dt\end{aligned} \tag{10}$$

where $\langle i^2\rangle_{\rm sig}, \langle i^2\rangle_{\rm sig\text{-}sp}$ and $\langle i^2\rangle_{\rm RIN}$ are, respectively, signal shot noise, signal-spontaneous beat noise and RIN. Note that the time dependence of signal-spontaneous beat noise has the same functional form as the well-known expression for signal shot noise.

To be compatible with the noise model in [16], the noise current due to RIN, which depends on the received optical intensity, had to be expressed in a form that explicitly accounts for the history of the received optical intensity, as well as the impulse response of the receiver. This was done by modeling RIN as a filtered-Poisson shot noise process with a time-dependent intensity function (mean rate of primary shot noise events) that is proportional to the square of received optical power. It should be noted that under steady-state conditions (constant received optical power) the signal-spontaneous beat noise reduces to that given by Olsson [17], and the spontaneous-spontaneous beat noise, too, reduces to that in [17] if it is assumed that $B_o \gg B_e$ so that $2B_o - B_e \approx 2B_o$, a condition that was assumed in the theory of [16]. The RIN, too, reduces to that expected for constant optical power. Relating the time-domain expressions for noise in (9) under steady-state conditions to their well-known forms, expressed in terms of NEB's and noise spectral densities, is straightforward if the following relationship is observed:

$$\begin{aligned}\sum_n h^2(\tau - n\Delta t)\Delta t &= \sum_n h^2(n\Delta t)\Delta t\\ &\approx \int |H(f)|^2\,df = 2B_e\end{aligned}$$

which follows directly from Parseval's theorem, where $H(f)$ is the receiver's transfer function and B_e is the one-sided NEB.

Bit error ratios (BER's) where calculated in an exhaustive manner, through

$${\rm BER} = \frac{1}{2N}\sum_{m=1}^{M-1}\sum_{k=1}^{N}{\rm erfc}\left(\frac{|I_{m,k} - I_{{\rm th},m}|}{\sqrt{2}\sigma_{m,k}}\right) \tag{11}$$

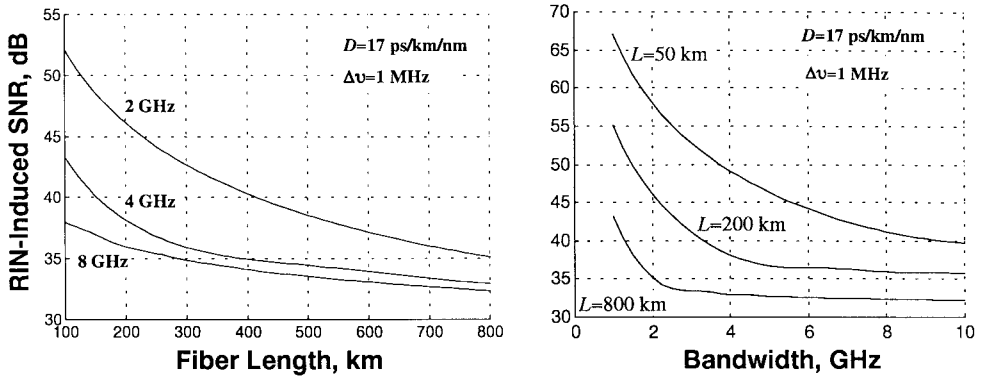
where M is the number of levels in a symbol, N is the number of symbols in the pseudonoise (PN) sequence, $I_{{\rm th},m}$ is the decision threshold of the mth decision circuit, $I_{m,k}$ is the expected value of the photocurrent during the kth symbol, and $\sigma_{m,k}$ is the standard deviation of the noise current, assumed to be a Gaussian random variable, for the kth symbol. In all cases, $I_{m,k}$ and $\sigma_{m,k}$ were calculated at an index n within each symbol that corresponded to the maximum eye opening. Because this was done independently for each eye in a multilevel signal, the index m is included in the subscript of $I_{m,k}$ and $\sigma_{m,k}$. For signals other than binary, (11) also includes the area in the tails of probability density functions (pdf's) belonging to symbols that are not adjacent to the threshold of a particular decision circuit; however, these contributions to the overall error probability would be very small and would have a negligible impact on the overall BER.

Receiver sensitivities were calculated by adjusting the received power until the target BER $= 10^{-9}$ was obtained. In all cases, $I_{{\rm th},m}$ was optimized according to a minimum BER criterion.

IV. Optimal Level Spacing in a 4-ary ASK Signal

Here we specifically consider the level spacing in a 4-ary ASK signal having equally-probable levels. Let the normalized weights for the 4-ary optical intensity be "0," $\varepsilon_1, \varepsilon_2$, and "1" where the lowest normalized weight, "0" corresponds to the symbol with minimum optical power (not necessarily zero optical power), and "1" corresponds to the symbol with the largest optical power. Then, ε_1 and ε_2 are the normalized weights for the second and third levels, respectively. Given that the noise in an optically preamplified receiver is strongly signal dependent, it is clear that the lowest probability of error will be achieved when unequal level spacing is used. For any optical extinction ratio, δ, it is easy to show that levels should be equally-spaced as {0, 1/3, 2/3, 1} when the noise is stationary, i.e., not signal dependent. This is the case, for example, when receiver thermal noise dominates. If the dominant noise is linearly proportional to received optical power, such as signal shot noise or signal-spontaneous beat noise, then, assuming an infinite extinction ratio, it can be shown that the optimal level weights become {0, 1/9, 4/9, 1}, i.e., they are quadratically spaced. If the extinction ratio is

Authorized licensed use limited to: University of Nevada Las Vegas. Downloaded on June 10,2023 at 20:47:21 UTC from IEEE Xplore. Restrictions apply. IPR2023-00838
Exhibit 2002
Page 4



(a) (b)

Fig. 5. (a) PM–AM RIN-induced SNR for various receiver bandwidths versus fiber length and (b) for various fiber lengths versus receiver bandwidth.

finite, the normalized weights approach those for stationary noise as the extinction ratio is degraded. When the dominant noise is RIN, i.e., is proportional to the square of received optical power, then the optimal weights for ε_1 and ε_2 become

$$\varepsilon_1 = \frac{\delta^{1/3} - 1}{\delta - 1}$$
$$\varepsilon_2 = \frac{\delta^{2/3} - 1}{\delta - 1} \tag{12}$$

which can be arrived at by observing the fact that optimal level spacing is obtained when the ratio of adjacent optical intensity levels is the same for all levels. Because the electrical signal power is proportional to the square of received optical power, the electrical signal-to-noise ratio (SNR) will be fixed when RIN dominates, with an associated BER floor. Obviously, it is desirable to keep the BER floor associated with RIN well below the target BER to avoid a RIN-induced power penalty, or a BER floor worse than the target BER.

V. Impact of RIN from PM–AM Noise Conversion

When a nonzero linewidth source is used over dispersive fiber, phase modulation (PM) to amplitude modulation (AM) noise conversion occurs, which can result in a significant RIN in the detected optical intensity [18], [19]. For long fiber lengths and/or wide bandwidths, PM-to-AM RIN can produce BER floors much worse than those desired in lightwave systems. Hence, it is important to consider this noise source in high-speed lightwave systems operating over SSF, especially when multilevel signaling is employed where a high SNR is required.

Yamamoto et al. derived an expression for the PM-to-AM RIN spectral density in terms of an infinite sum of Bessel functions, expressed as (19) in [18]. For frequencies above a few hundred kHz and source linewidths no greater than a few hundred MHz, which encompasses the wide range of parameters of practical interest, only the zero and first-order Bessel functions contribute significantly to the RIN spectral density, and (19) in [18] can be expressed in a simplified form, as

$$N(f) = \frac{4\Delta\upsilon}{\pi f^2} \sin^2(4\pi^2 F_D f^2) \tag{13}$$

where $\Delta\upsilon$ is the source linewidth and F_D is a dispersion parameter, given by

$$F_D = \frac{\lambda^2}{4\pi c} DL. \tag{14}$$

Note that for optically compensated systems the extent of PM-to-AM noise conversion would be greatly reduced since $D \approx 0$ ps/(km·nm). It is also interesting to note that for shorter fiber lengths and/or smaller bandwidths, i.e., $\sin(x) \approx x$ in (13), (13) reduces to the expression derived by Petermann in [19].

Assuming a receiver with an ideal brick-wall response with bandwidth B_e, (13) can be integrated to get the total RIN in the bandwidth of the receiver, as

$$\text{RIN}_{\text{PM,AM}} = \frac{2\Delta\upsilon}{\pi B_e}[\cos(8\pi^2 F_D B_e^2) + 4\pi^{2/3} B_e \sqrt{F_D}\ \text{FresnelS}\ (4B_e\sqrt{\pi F_D}) - 1] \tag{15}$$

where FresnelS is the Fresnel sine function. From (15) it can be seen that the total RIN scales linearly with the source linewidth, but shows a more complicated dependence on the receiver bandwidth and fiber length. As an example, Fig. 5 shows the PM–AM RIN-induced SNR (i.e., 1/RIN) versus fiber length and receiver bandwidth for a laser source with a 1 MHz linewidth.

Recall from the previous section that when RIN dominates, the probability of error is minimized when the ratio of adjacent levels is the same for all levels in an M-ary signal. When the level spacing is not optimal, then the two levels that form the smallest ratio $k_{\min}$ will dictate the BER. For a given amount of RIN and ratio $k_{\min}$, the BER can be obtained from

$$Q_x = \frac{1}{\sqrt{\text{RIN}}}\left[\frac{k_{\min} - 1}{k_{\min} + 1}\right] \tag{16}$$

where Q_x relates to the BER of an M-level signal, through

$$\text{BER} = \frac{(M-1)}{M}\ \text{erfc}\left(\frac{Q_x}{\sqrt{w}}\right). \tag{17}$$

In (17) it was assumed that the BER of a decoded binary tributary is the same as the symbol-error ratio of the M-ary signal, and that the level spacing is optimized so that the

A. Soto and W. Soto
Authorized licensed use limited to: University of Nevada Las Vegas. Downloaded on June 10,2023 at 20:47:21 UTC from IEEE Xplore. Restrictions apply. IPR2023-00838
Exhibit 2002
Page 5

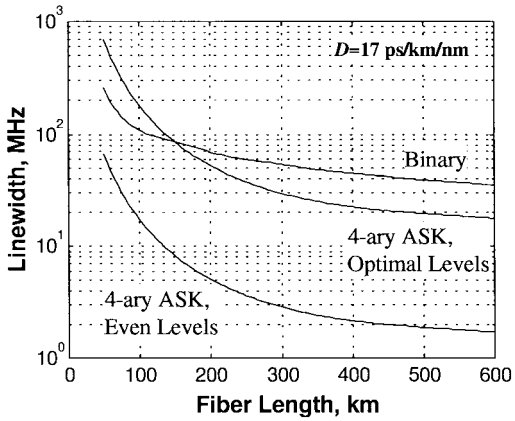


Fig. 6. Linewidth that will produce a 10^{-14} BER floor due to PM–AM RIN noise for 10 Gb/s transmission.

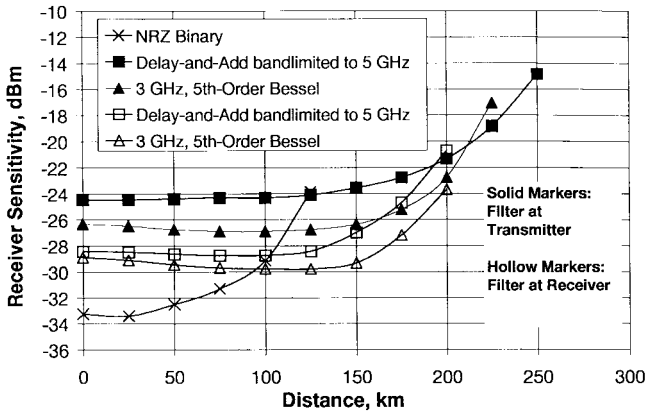


Fig. 7. Receiver sensitivity versus distance for an NRZ binary signal and for systems employing a duobinary filter at the transmitter or receiver. Delay-and-add filters were bandlimited using a 5-GHz, twelfth-order Butterworth low-pass filter.

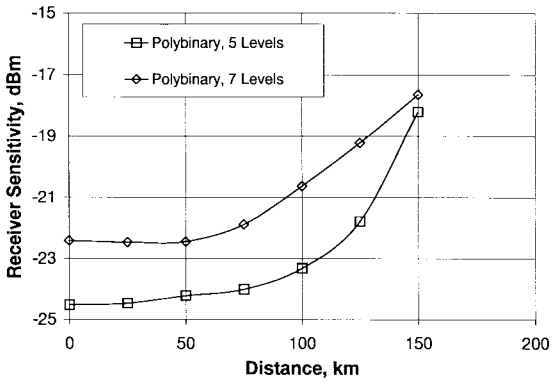


Fig. 8. Receiver sensitivity versus distance for five- and seven-level polybinary signals.

probability of error is the same for all levels. In the limiting case of nonoptimal level weights in which only the two levels that make up the ratio $k_{\min}$ contribute to the error probability, the coefficient of the complementary error function in (17) becomes $1/M$; hence (17) overestimates the BER by at most a factor $M-1$.

Using (15)–(17), the source linewidth for a given BER floor can be determined. For example, Fig. 6 shows the source linewidth that will produce BER $= 10^{-14}$ for a binary signal, and for a 4-ary ASK signal with equally-spaced and optimally spaced levels. Note that ideal levels (zero ISI) are assumed in Fig. 6, i.e., only the effects of PM–AM noise conversion are considered, and not distortion from chromatic dispersion. In all cases, a receiver bandwidth equal to 70% of the symbol rate was assumed in Fig. 6. A 4-ary ASK signal with optimal level weights is actually more robust than a binary signal at shorter distances because of a reduced receiver bandwidth. Recall from Fig. 5 that PM–AM RIN depends strongly on the receiver bandwidth at shorter distances.

VI. Simulation Results

Simulation results are presented in this section for an optically-preamplified system using the various multilevel signaling schemes. In all cases, an EDFA preamplifier with a 25 dB gain, 1.5 dB input insertion loss, and a spontaneous emission factor of 2 (6-dB noise figure) is assumed. The ASE is filtered by a 1.5 nm optical bandpass filter. A fiber dispersion of 17 ps/(km·nm) is used, and the electrical receiver response, unless specified otherwise, is taken as a third-order Butterworth filter with a 3-dB cutoff at 65% of the symbol rate. Unless specified otherwise, all results assume an ideal source (0 Hz linewidth) and a $LiNbO_3$ external modulator with a balanced drive and ideal (infinite) dc extinction ratio.

A. Polybinary Signals

A polybinary filter can be placed at the transmitter to obtain a multilevel, intensity-modulated polybinary signal, or at the receiver where the detected binary, intensity-modulated signal is converted to a multilevel polybinary signal. Because of the nonlinear nature from electrical input to electrical output of the system considered here, the most suitable point within the system to implement the polybinary filter is not obvious. Fig. 7 shows the receiver's sensitivity for a 10-Gb/s system using duobinary signaling, with a duobinary filter placed at either the transmitter or receiver. A result is also shown for a conventional binary signal. A duobinary filter can be realized with a delay-and-add filter, or with a lowpass filter having a cutoff at ~0.25–0.3 times the bit rate—Bessel filters work particularly well in generating a duobinary signal from an NRZ binary input. When a delay-and-add filter is used, it is imperative to bandlimit the duobinary signal to one-half the bit rate (as was done for the results in Fig. 7 using a 5 GHz, twelfth-order Butterworth filter) in order to obtain an improvement in the dispersion-limited distance [20]. From Fig. 7 it can be seen that a duobinary filter at the receiver offers consistently better system reach than a filter placed at the transmitter largely because the baseline sensitivity (i.e., that at zero distance) is about 2 dB better when placing the duobinary filter at the receiver because the continuous rolloff of the duobinary filter response offers a lower noise equivalent bandwidth (NEB), with an associated decrease in the amount of noise.

Simulations were also performed for five- and seven-level polybinary signals, as shown in Fig. 8. The results in Fig. 8

A. Soto and W. Soto
Authorized licensed use limited to: University of Nevada Las Vegas. Downloaded on June 10,2023 at 20:47:21 UTC from IEEE Xplore. Restrictions apply. IPR2023-00838
Exhibit 2002
Page 6

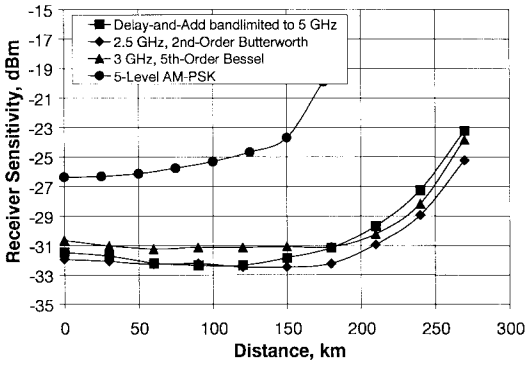


Fig. 9. Receiver sensitivity versus distance for AM-PSK polybinary signals using various duobinary filters at the transmitter. The delay-and-add filter was bandlimited by a 5-GHz, twelfth-order Butterworth low-pass filter.

are for systems using a polybinary filter at the receiver only. As with duobinary signals, it was found that a polybinary filter at the receiver offered consistently better system reach than a filter placed at the transmitter because of the reduced NEB of the receiver. Polybinary signals were generated using an ideal delay-and-add polybinary filter in cascade with a 5 GHz, twelfth-order Butterworth filter to bandlimit the signal. It was found that, although higher-order polybinary signals concentrate the PSD at frequencies closer to the optical carrier, they require the same transmission bandwidth as a duobinary signal. If a polybinary signal is bandlimited to less than one-half the bit rate, it is not possible to obtain a signal without ISI. This minimum bandwidth requirement is fundamentally linked to the symbol period of a polybinary signal, which, regardless of the number of levels, is always equal to the bit period [24]. Also, because of the increased number of levels, higher order polybinary signals possess an inherent power penalty, and tend to be more susceptible to distortion from chromatic dispersion than a duobinary signal.

B. AM-PSK Polybinary Signals

Simulated results of receiver sensitivity versus distance are shown in Fig. 9 for an optical AM-PSK duobinary signal in which the duobinary filter at the transmitter is implemented by 1) a delay-and-add filter bandlimited to one-half the bit rate by a 5 GHz twelfth-order Butterworth response, 2) a 2.5-GHz second-order Butterworth filter, and 3) a 3-GHz fifth-order Bessel response. A result is also shown in which a five-level polybinary signal is applied to the MZ biased at maximum extinction to produce an optical AM-PSK polybinary signal with three intensity levels. The five-level polybinary signal was generated using an ideal delay-and-add polybinary filter in cascade with a 5-GHz, twelfth-order Butterworth filter. It can be seen that no improvement is offered for the higher-level optical AM-PSK polybinary signal. As with the conventional polybinary signals discussed in the previous section, higher order AM-PSK polybinary signals do not allow the transmission bandwidth to be reduced further compared to an AM-PSK duobinary signal, but only result in more intensity levels, thereby introducing an inherent power penalty and making the signal more susceptible to distortion from chromatic dispersion.

Note that bandlimiting the electrical duobinary signal applied to the MZ is essential to obtain an improved dispersion tolerance in an AM-PSK duobinary signal [20]. This can be achieved by following the delay-and-add filter with a bandlimiting filter, or by using a low-pass filter to approximate a bandlimited duobinary filter. Note that bandlimiting the signal applied to the MZ suppresses higher order spectral lobes about the carrier that would otherwise undergo severe phase distortion and increase the nonlinear intensity-envelope distortion falling within the bandwidth of the receiver—the receiver bandwidth is the same for binary and AM-PSK duobinary signals. Removing higher order lobes can be achieved by bandlimiting the optical field with a bandpass filter, but is more easily achieved by bandlimiting the electrical signal applied to the modulator, as shown in Fig. 10. A different, but interesting interpretation of the electrical filter requirements for an optical AM-PSK duobinary signal is given in [23].

C. M-ary ASK and Polyquaternary Signals

Unlike polybinary signals, M-ary ASK signals possess a symbol period that is increased by a factor $\log_2(M)$ compared to a binary or polybinary signal operating at the same bit rate and, consequently, the transmission bandwidth is reduced by a factor $1/\log_2(M)$. Fig. 11 shows receiver sensitivity versus distance for a 4- and 8-ary ASK signal, as well as for a seven-level polyquaternary signal in which the partial response filter was implemented at the receiver using a 1.5 GHz, fifth-order Bessel filter. For these simulations, the level spacing was approximately equal for the transmitted optical power. The 1-dB dispersion-limited distance is, respectively, $\sim$200, 300, and 450 km for the 4-ary ASK, polyquaternary and 8-ary ASK signals. The baseline sensitivity, however, is significantly degraded for these signals because of an increased number of levels and the signal dependence of signal-spontaneous beat noise. In the presence of stationary noise only, and assuming a white noise spectral density, it is straightforward to show that the additional optical power required for an M-ary ASK signal over a binary signal is

$$P_M = \frac{M-1}{\sqrt{\log_2(M)}}. \tag{18}$$

According to (18) a 4-ary ASK signal would require about 3.3 dB more optical power than a binary signal. When an EDFA preamplifier is used, however, the signal dependence of signal-spontaneous beat noise increases the penalty substantially to about 8 dB, assuming equally spaced levels, and to about 5 dB when the levels are optimally spaced.

Obtaining optimal level spacing may not be practical in an M-ary signal because the temporal width of the lowest eye is reduced significantly when the M-ary signal is bandlimited at the transmitter and/or receiver. Furthermore, a very small vertical opening in the bottom eye makes it more susceptible to chromatic dispersion; hence, level spacing that is optimal in the absence of dispersion is not likely optimal when dispersion is included.

It is interesting to conjecture that for Gb/s data-rate systems operating over bandlimited multimode fiber with PIN

A. Soto and W. Soto
Authorized licensed use limited to: University of Nevada Las Vegas. Downloaded on June 10,2023 at 20:47:21 UTC from IEEE Xplore. Restrictions apply. IPR2023-00838
Exhibit 2002
Page 7

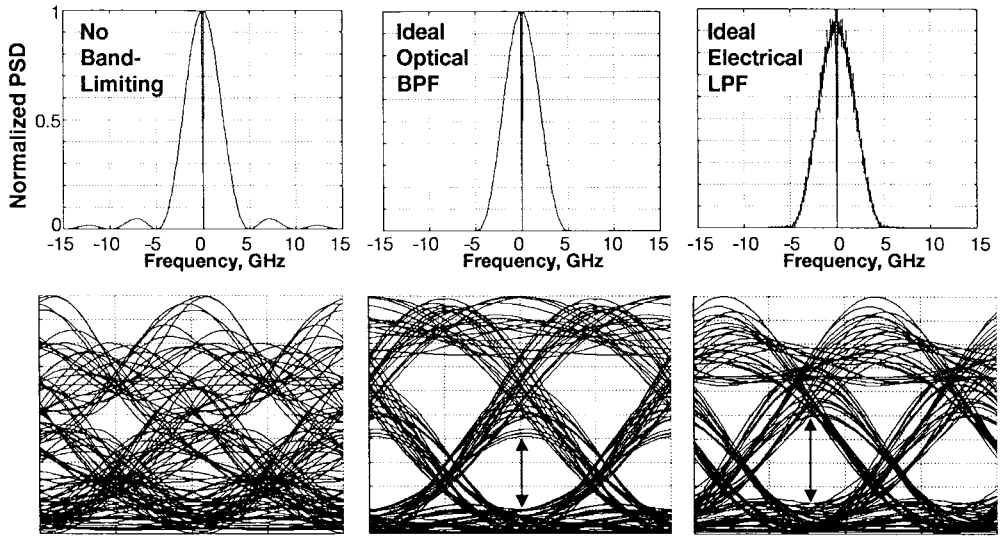


Fig. 10. PSD of the optical electric field (top) and corresponding filtered receiver eye diagrams (bottom) after transmission over 200 km for an optical AM-PSK duobianry signal.

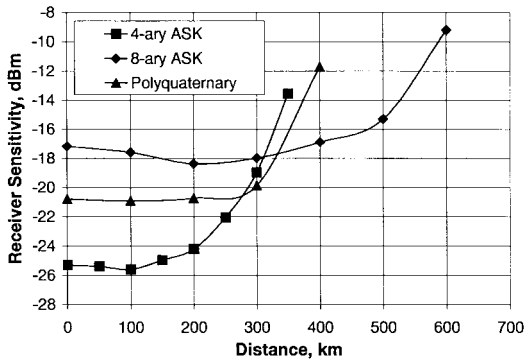


Fig. 11. Receiver sensitivity versus distance for 4-ary ASK, 8-ary ASK, and polyquaternary (seven levels) signals.

receivers and no optical amplifiers, M-ary ASK could provide bandwidth relief.

D. Effect of External Modulator Frequency Chirp

Any real MZ will possess a finite dc optical extinction ratio, which will give rise to a residual chirp in the transmitted signal [15]. For signaling formats in which the MZ is biased at the half-power point of its transfer characteristic, such as binary, M-ary ASK and polybinary, the residual chirp polarity will be either positive or negative. A negative chirp polarity is usually desired because it produces a red shift on the rising edge of optical pulses and a blue shift on the falling edge, which gives rise to pulse compression over a certain range of distances, thereby improving the dispersion tolerance of the signal. Positive residual chirp has the opposite effect and can degrade the performance significantly. For an AM-PSK duobinary signal, the polarity of residual chirp alternates when marks are separated by an odd number of spaces [15]. Fig. 12 shows the effect of residual chirp on various signaling schemes where it can be seen that systems using binary, 4-ary ASK, or a duobinary receiver benefit from some amount of negative residual chirp. The performance of an AM-PSK duobinary signal, however, is always degraded. Hence, an MZ with a high dc extinction ratio should be used with an AM-PSK duobinary signal. If positive residual chirp is present for any of the other signaling schemes, it is always possible to reverse the chirp polarity by simply changing the dc bias by $\pm V_\pi$.

It is also possible to control the chirp on an external modulator by adjusting the weights of the electrical signals applied to each electrode of a dual-drive MZ [21], [22]. Fig. 13 shows receiver sensitivity versus chirp parameter for a binary signal and an MZ possessing various amounts of residual chirp, i.e., different dc extinction ratios. The chirp parameter is defined in terms of the peak-to-peak amplitudes, V_1 and V_2, applied to each arm of the MZ, through

$$\alpha = \frac{V_2 + V_1}{V_2 - V_1} \tag{19}$$

For an ideal MZ, i.e., infinite DC extinction ratio, a chirp of $\alpha = -1$ is optimal, and a significant benefit is obtained compared to $\alpha = 0$ at longer distances. When there is negative residual chirp, however, the optimal controlled negative chirp decreases as the residual chirp increases from an increasing dc extinction ratio. If the residual chirp is positive, then a larger negative controlled chirp is required to offset the deleterious positive residual chirp.

Fig. 14 shows receiver sensitivity versus chirp parameter for a 4-ary ASK signal where, again, a benefit is obtained for negative residual chirp, although a chirp of $\alpha = -0.3$ is optimal for distances greater than about 200 km. In the presence of negative residual chirp, the optimal controlled chirp moves closer to zero, just as for a binary signal. It is apparent from Figs. 13 and 14 that the benefit from controlled frequency chirping is reduced when there is negative residual chirp already present. An AM-PSK duobinary signal does not benefit from the controlled frequency chirping imparted by an unbalanced drive because the chirp polarity, just as with residual chirp, alternates on marks separated by an odd number of spaces. Hence, it is important to use a balanced drive with an AM-PSK duobinary signal.

A. Soto and W. Soto
Authorized licensed use limited to: University of Nevada Las Vegas. Downloaded on June 10,2023 at 20:47:21 UTC from IEEE Xplore. Restrictions apply. IPR2023-00838
Exhibit 2002
Page 8

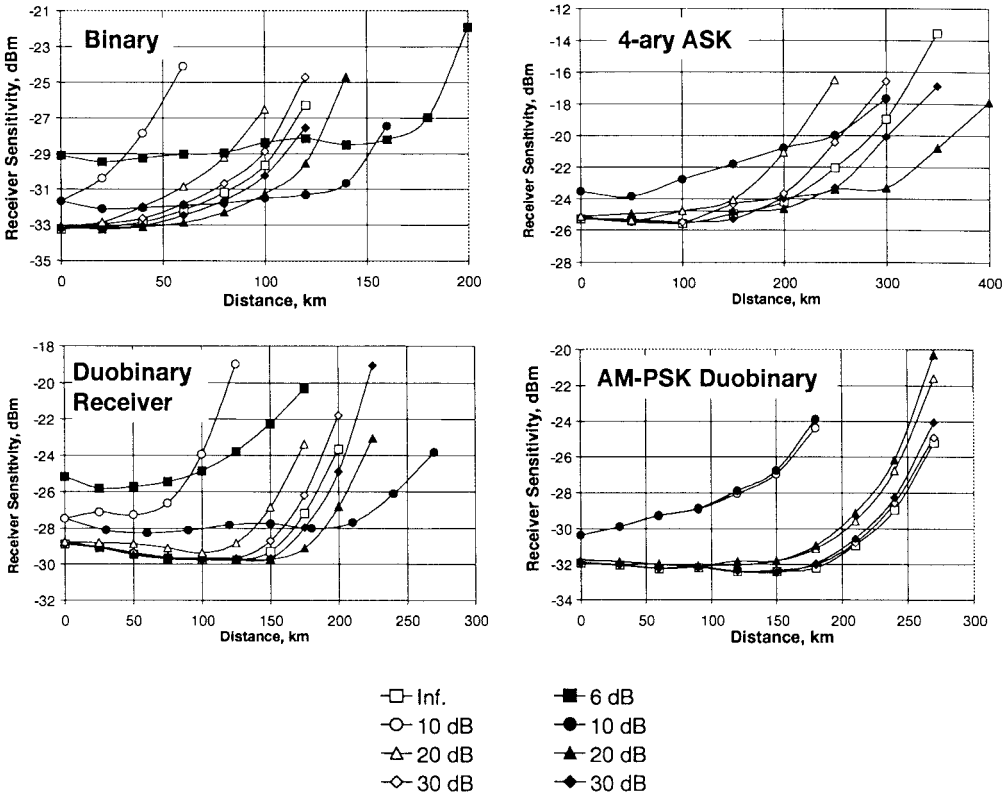


Fig. 12. Effect of residual chirp from a finite dc optical extinction ratio on various signaling schemes. Hollow markers with finite extinction ratio denote positive residual chirp. Solid markers denote negative residual chirp.

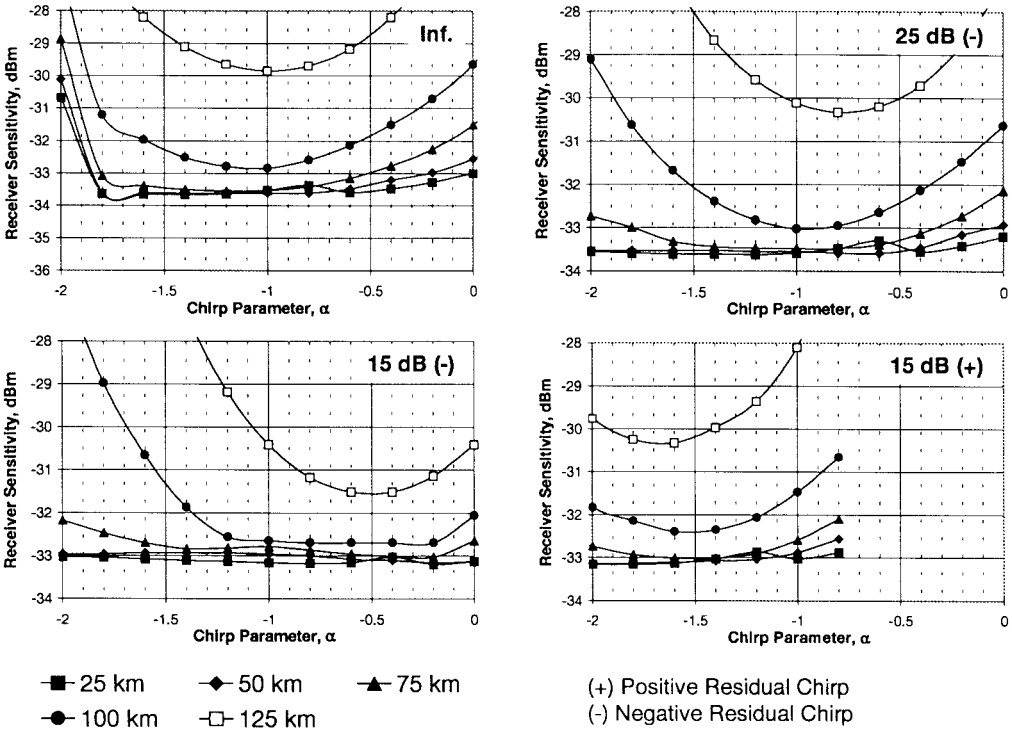


Fig. 13. Receiver sensitivity versus chirp parameter for a binary system using an external modulator with various dc extinction ratios and residual chirp polarity.

E. Overview of Expected Reach for Signaling Schemes

A comparison of the various signaling schemes may favor one format over an other depending on the system parameters used in evaluating performance. Some useful conclusions, however, can be made. For example, polybinary signals with more than three levels are of little practical use because they do not allow for a further reduction in the required bandwidth over a duobinary signal. It is also clear that for a conventional

A. Soto and W. Soto
Authorized licensed use limited to: University of Nevada Las Vegas. Downloaded on June 10,2023 at 20:47:21 UTC from IEEE Xplore. Restrictions apply. IPR2023-00838
Exhibit 2002
Page 9

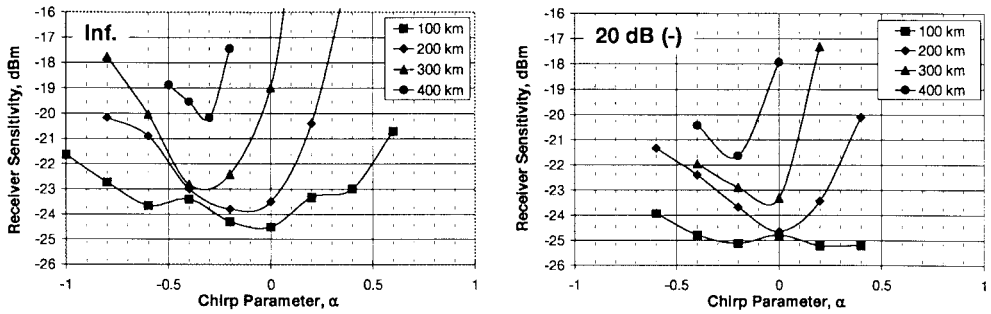


Fig. 14. Receiver sensitivity versus chirp parameter for a 4-ary ASK system using an external modulator with an ideal and 20 dB dc extinction ratio.

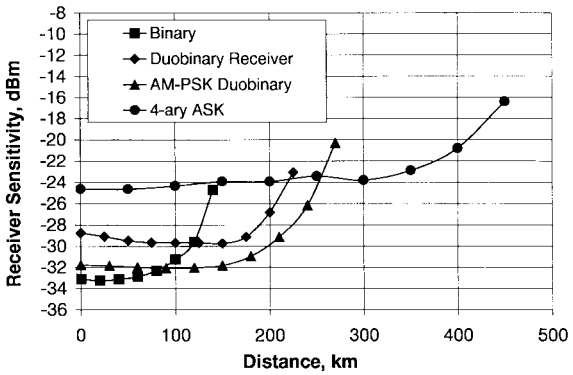


Fig. 15. Receiver sensitivity versus distance for various signaling schemes.

duobinary signal, the duobinary filter should be implemented at the receiver to obtain a lower NEB and, therefore, an improved baseline sensitivity. To be fair, a practical set of parameters should be assumed when making a comparison. For example, a dc optical extinction ratio of 20 dB is reasonable for an MZ device. Negative residual chirp is also a reasonable assumption because it can always be obtained by appropriately setting the MZ's bias point. Under these conditions, Fig. 15 shows receiver sensitivity for the most promising schemes. For distances up to about 100 km, conventional binary signaling with negative residual chirp is adequate. For distances from 100 to 200 km, the AM-PSK duobinary signal is best suited and would likely be favored over a duobinary receiver because of the lower baseline sensitivity and a simpler implementation. The 4-ary ASK signal may be suited for distances between 200 and 350 km. Although it has the disadvantage of a much higher baseline sensitivity, a 4-ary ASK signal has the advantage that all logic components at the transmitter and receiver are required to operate at only one-half the bit rate. Higher level M-ary signals or the polyquaternary signals are not likely to be practical because of the excessively large power required at the receiver. Signals with more levels are also more susceptible to the nonideal frequency response of components. Issues concerning fiber nonlinearities would also have to be carefully studied for these signals.

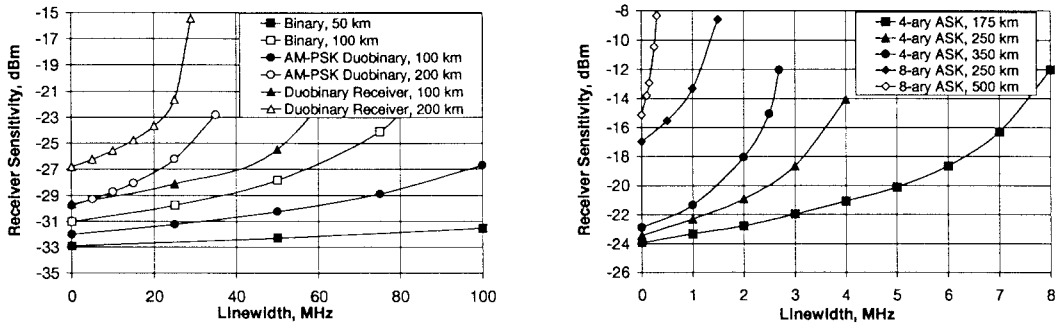
F. Power Penalty from a Nonzero Source Linewidth

In Fig. 6 the impact of PM-to-AM RIN for a nonzero source linewidth was considered for ideal (zero ISI) signals. When dispersion is included, it is clear that eye closure will significantly increase the impact of PM–AM RIN, and that narrower linewidths will be required at a given distance to reduce the impact of this noise source. Fig. 16 shows receiver sensitivity versus linewidth for the different signaling schemes at various distances, including the effects of fiber dispersion. Assuming a maximum allowable PM–AM RIN-induced power penalty of 2 dB, a binary signal can tolerate a source linewidth as high as about 100 and 40 MHz when transmitting over 50 and 100 km, respectively. For the AM-PSK duobinary signal, the linewidth must be no greater than about 50 and 20 MHz, respectively, when transmitting over 100 and 200 km. For a system using a duobinary filter at the receiver, the linewidth requirements are reduced to around 30 and 15 MHz when transmitting over 100 and 200 km, respectively. A linewidth no greater than about 3, 1.5, and 1 MHz is required for the 4-ary ASK signal when transmitting over 175, 250, and 350 km, respectively. An 8-ary ASK signal requires a very narrow linewidth of about 700 kHz for transmission over 250 km, and 150 kHz for transmission over 500 km. This is yet another reason higher level M-ary signals may not be practical for long-haul transmission.

G. Optical Inline Amplifiers and ASE Accumulation

For an AM-PSK duobinary signal, the full $\sim$200 km can be spanned without the use of inline EDFA's, or possibly using one inline EDFA in a more practical situation. For a 4- or 8-ary ASK signal, however, inline EDFA's are certainly required because of the larger received power required and the additional fiber loss for transmission beyond 200 km. To investigate the impact of ASE accumulation, Fig. 17 shows BER versus launched optical power, i.e., power launched into the fiber, for 4- and 8-ary ASK signals with an amplifier spacing of 40 and 80 km. A 20-dB dc extinction ratio is assumed for the MZ with negative residual chirp. These results assume that the gain of inline EDFA's exactly balance the interlink loss, assumed to be 16 and 28 dB for 40 and 80 km links, respectively, and do not account for fiber nonlinearities. The interlink loss values assume a 2-dB insertion loss at the input and at the output of each inline amplifier, a fiber loss of 0.25 dB/km, and splice losses of 0.05 dB/km. A 6-dB noise figure is assumed for each inline amplifier. If it is assumed that the launched optical power should not exceed, say, $+10$ dBm to avoid significant fiber nonlinear effects, then amplifiers would have to be placed no more than about 80 km apart for a 4-ary ASK signal transmitted over 320 km. For

A. Soto and W. Soto
Authorized licensed use limited to: University of Nevada Las Vegas. Downloaded on June 10,2023 at 20:47:21 UTC from IEEE Xplore. Restrictions apply. IPR2023-00838
Exhibit 2002
Page 10



(a) (b)

Fig. 16. Receiver sensitivity versus source linewidth: (a) binary and duobinary systems and (b) M-ary ASK systems.

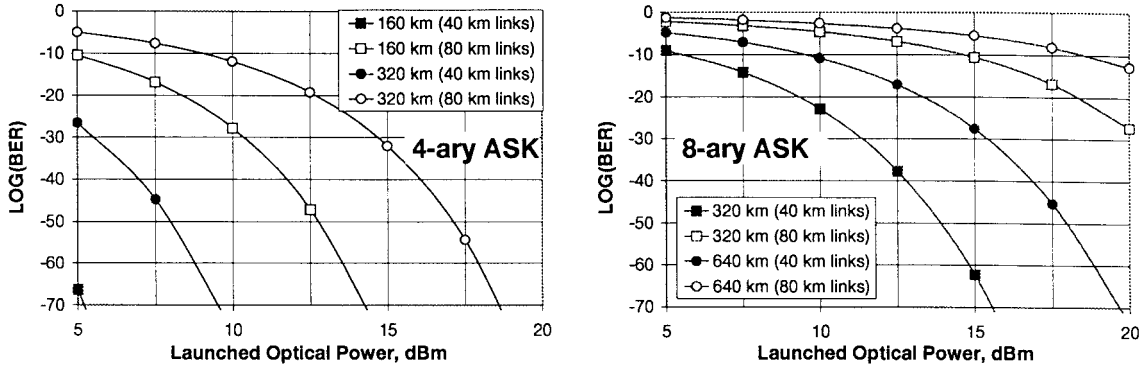


Fig. 17. BER versus launched optical power for 4–ary ASK and 8-ary ASK signals.

an 8-ary ASK signal, amplifiers would have to be spaced no more than about 40 km apart for transmission over 640 km of fiber. Moreover, fiber nonlinearities would likely restrict transmission of an 8-ary ASK signal over such a long distance if the launched power were to approach +10 dBm. For 80 km amplifier spacing, the 8-ary ASK signal would require a launched power of at least +15 and +20 dBm, respectively, when transmitting over 320 and 640 km. Clearly, these powers preclude the use of higher level signaling schemes.

For any distance and set of receiver parameters, the required ratio of optical signal power to ASE power incident on the photodetector for a target BER can be calculated for a system using an optical preamplifier only, i.e., no inline amplifiers. Then, when an optical postamplifier and inline amplifiers are added, the same target BER will be achievable provided the ratio of signal to ASE power is maintained. In other words, as the ASE is increased due to ASE accumulation, the signal power must also be increased at the receiver to maintain the signal-to-ASE power ratio. The amount by which the signal power must be increased is the incurred penalty for using inline amplifiers. For the parameters used in simulations, which includes the use of a 1.5 nm optical bandpass filter, signal-to-ASE power ratios of ∼6, 14, and 22 dB are required for binary, 4-ary ASK and 8-ary ASK signals, respectively.

VII. Experimental Results

The 10 Gb/s 4-ary ASK transmission experiments were conducted using two transmitters: a) for distances up to 170 km using an integrated III–V laser and MZ modulator module whose laser had a linewidth of 35 MHz, and b) for distances up to 225 km using a discrete $LiNbO_3$ MZ with a laser whose linewidth was 4 MHz. BER versus received optical power is shown in Fig. 18 for experiments using the III–V MZ and 35 MHz linewidth laser. Measured receiver sensitivities at 0 km for BER $= 10^{-9}$ were −15.8 and −12.5 dBm, respectively, for a system with and without optical preamplification. Simulated results predict a sensitivity to within 2 dB of experimental results at 0 km. Note that only a marginal improvement in sensitivity was obtained using the optical preamp because it had a low gain of ∼8 dB and an output insertion loss of 3.8 dB at 1557 nm, which was

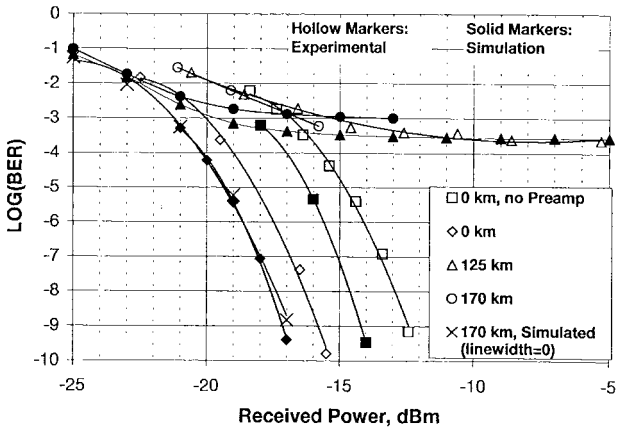


Fig. 18. BER versus received optical power for 4-ary ASK experiments using a III–V MZ module.

A. Soto and W. Soto
Authorized licensed use limited to: University of Nevada Las Vegas. Downloaded on June 10,2023 at 20:47:21 UTC from IEEE Xplore. Restrictions apply. IPR2023-00838
Exhibit 2002
Page 11

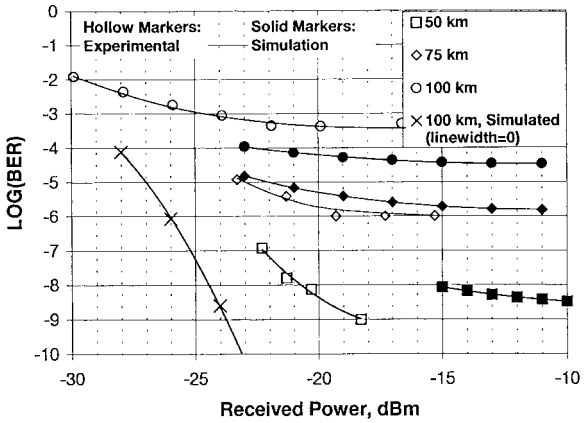


Fig. 19. BER versus received optical power for 4-ary ASK experiments using a III–V MZ module, and two EDFA's in cascade as an optical preamplifier.

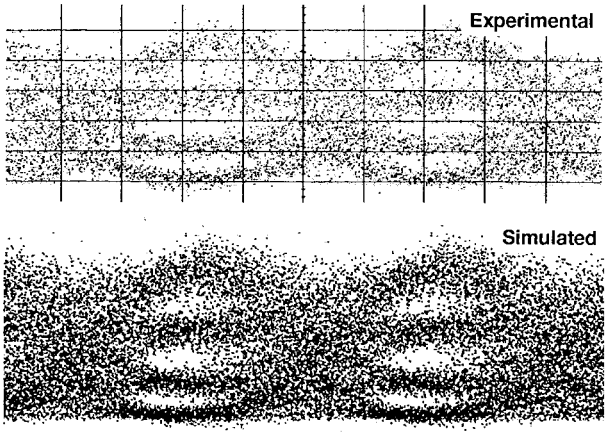


Fig. 20. Experimental and simulated eye diagrams for a 4-ary ASK signal transmitted over 170 km.

the emission wavelength of the laser built into the III–V MZ module. The average launched power was +8.2 dBm for these experiments. At 125 and 170 km, BER floors are clearly present, which were also predicted by simulation results due to PM-to-AM noise conversion resulting from the 35 MHz linewidth laser. The linewidth of the laser was measured to be ~35 MHz using the delayed self-homodyne (DSH) technique, and this value was used in simulating the amount of PM–AM RIN. A simulation result is also shown at 170 km in Fig. 18 for an ideal source, i.e., 0 Hz linewidth. Results are shown in Fig. 19 for another set of experiments that used only an optical preamp and postamp. For these experiments, two EDFA's were used in cascade at the receiver to obtain a higher gain of ~18 dB. Although BER $= 10^{-9}$ was possible at 50 km, the BER curve shows signs of bending toward a BER floor. For transmission over 75 km an error floor of $\sim 10^{-6}$ was observed, and was also predicted from simulations due to PM-to-AM noise conversion. At 100 km the error floor observed was between 10^{-3} and 10^{-4}. Also shown in Fig. 19 is a simulation result at 100 km that excludes PM-to-AM RIN by assuming an ideal source.

Simulated and experimental eye diagrams are shown in Fig. 20 for the received 4-ary signal after transmission over

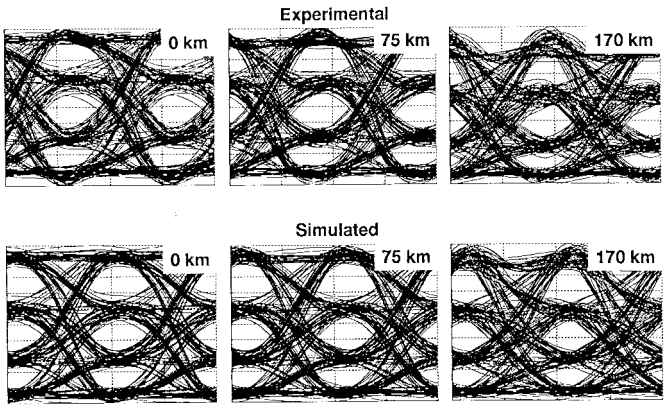


Fig. 21. Experimental and simulated eye diagrams for 10 Gb/s 4-ary ASK experiments using a III–V MZ module.

170 km. Note that the simulated result has noise superimposed to make a more direct comparison to the eye diagram observed on the digital oscilloscope. Although a highly signal-dependent noise appears to be present in these eye diagrams, it is difficult to determine whether a particular sample within an eye is due to noise, or due to a deviant trace. To obtain much more detail, measured eye diagrams were constructed from acquired time records of the entire PN sequence, but with the effects of noise greatly reduced by setting the oscilloscope to a time-averaging mode in which each sample is the average of multiple samples taken at the same point in time relative to the start of the PN sequence. The experimental time-averaged eye diagrams at various distances are shown in Fig. 21, along with simulated eye diagrams in the absence of noise. For the simulations we used acquired experimental time records for the PN sequence applied at the transmitter, as well as acquired frequency response records (magnitude and phase) for devices such as electrical amplifiers, filters, external modulators, and photodetectors. Much more detail about ISI is provided by acquiring eye diagrams using the time-averaging technique, as can be seen by contrasting the result at 170 km in Fig. 21 with Fig. 20.

A third set of experiments were conducted using a laser source with a 4 MHz linewidth and a $LiNbO_3$ MZ with a balanced drive. Fig. 22 shows BER versus received power at various distances. The average launched power was +11.7 dBm for these experiments. The simulation results predict a receiver sensitivity to within 2 dB of those measured at 0 and 75 km. Unlike the experiments using the III–V module with the 35 MHz linewidth laser, however, the simulation predicts receiver sensitivities that are worse than those measured, possibly due to uncertainties in the MZ's bias point. An EDFA preamplifier and postamplifier were used for all the results in Fig. 22. An inline amplifier was placed at 75 km for the 150 km experiment, and at 75 and 150 km for the 225 km experiment. The gain of the EDFA preamplifier was about 23 dB (opposed to 8 dB when using the III–V module) at the 1538 nm wavelength of the 4 MHz laser; hence, a significant improvement in the receiver's sensitivity at 0 km was observed compared to experiments using the III–V MZ module. Furthermore, BER $= 10^{-9}$ was possible for distances up to 150 km

A. Soto and W. Soto
Authorized licensed use limited to: University of Nevada Las Vegas. Downloaded on June 10,2023 at 20:47:21 UTC from IEEE Xplore. Restrictions apply. IPR2023-00838
Exhibit 2002
Page 12

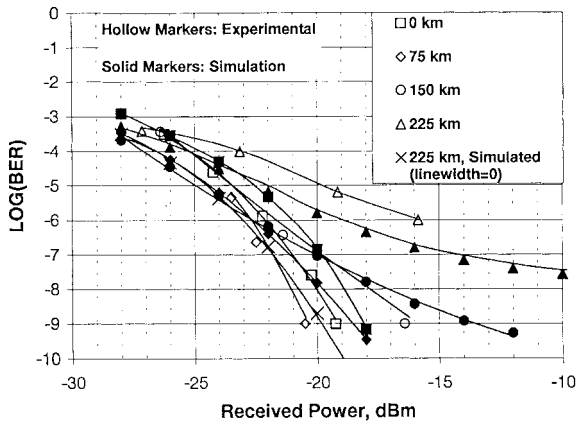


Fig. 22. BER versus received optical power for experiments using a dual-drive $LiNbO_3$ MZ and a narrow-linewidth laser.

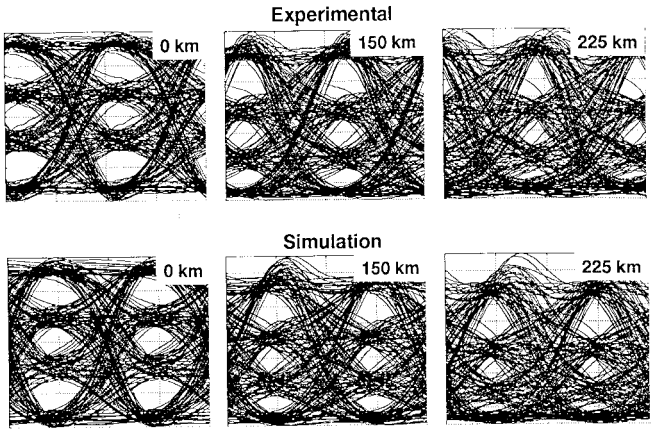


Fig. 23. Experimental and simulted eye diagrams for 10 Gb/s 4-ary ASK experiments using an $LiNbO_3$ MZ modulator.

for these experiments because of the narrower linewidth of the source, and the accompanying reduction in PM-to-AM RIN. Bending of the BER curve toward an error floor appears at the 150 km distance. For transmission over 225 km, BER $= 10^{-6}$ was possible for the available power, and the BER curve also bends toward an error floor. Simulation results predict a PM–AM RIN-induced error floor at about 10^{-8} when transmitting over 225 km. A simulation result is also shown in Fig. 22 for an ideal source. Experimental and simulated eye diagrams are shown in Fig. 23 at various distances indicating good agreement between simulation and experiment.

VIII. Conclusions

Multilevel signaling can be used to extend the dispersion-limited transmission distance in 10 Gb/s lightwave systems operating at ~1550 nm over standard fiber. Duobinary signaling allows the spectral occupancy to be bandlimited to about one-half that of a conventional binary signal, with an associated improvement in dispersion tolerance, making transmission up to ~200 km possible. For AM-PSK duobinary transmission it is essential that the electrical duobinary signal be bandlimited to one-half the bit rate to obtain the expected benefit. For duobinary intensity modulated signals, it was found that placing a duobinary filter at the receiver offers consistently better performance than placing the duobinary filter at the transmitter. Higher-level polybinary signals do not offer a further improvement in the dispersion-limited distance because, although they concentrate power closer to the carrier, they do not allow the spectral occupancy to be further reduced over a duobinary signal, and it is the required spectral occupancy that is the important parameter for assessing the dispersion tolerance of polybinary signals. Optical AM-PSK duobinary signaling is the best format of all the duobinary systems investigated because of its simple implementation, superior receiver sensitivity, and compatibility with a standard receiver.

The residual chirp accompanying an MZ with a finite dc optical extinction ratio can benefit binary, duobinary and M-ary ASK signaling schemes, provided the bias point on the MZ is set to give a negative chirp polarity. For an optical AM-PSK duobinary signal the residual chirp will always degrade performance and, therefore, it is important to use an MZ with a high dc extinction ratio. Furthermore, a balanced drive should be used with an AM-PSK duobinary signal to avoid degraded performance from an alternating chirp polarity. For binary, duobinary and M-ary ASK signals, controlled frequency chirping introduced through an asymmetric drive can extend the dispersion-limited distance; however, the benefit obtained becomes less significant when negative residual chirp is already present. In addition, the optimum chirp parameter depends on the amount of residual chirp that is present, which in turn depends on the dc extinction ratio of the MZ.

A 10 Gb/s 4-ary ASK signal can extend the transmission distance to about ~350 km, assuming a MZ modulator with a dc extinction ratio of 20 dB and negative residual chirp. Because of an increased number of levels and the signal dependence of signal-spontaneous beat noise, a 4-ary ASK signal requires about 8 dB more power than a binary signal. To maintain the required signal-to-ASE power ratio, amplifier spacing of no more than about 80 km is needed for a 10 Gb/s 4-ary ASK signal when the launched power is +10 dBm.

RIN from PM-to-AM noise conversion can result in significant power penalties or BER floors when transmitting over long distances of SMF. This noise scales linearly with the source linewidth and, therefore, it is important to use narrow linewidth sources, especially for multilevel signals where higher SNR's are required. To keep the PM–AM RIN-induced power penalty to below 2 dB when transmitting a 10 Gb/s 4-ary ASK signal over 200–300 km, the source linewidth must be no greater than about 1 MHz.

References

[1] G. May *et al.*, "Extended 10 Gb/s fiber transmission distance at 1538 nm using a duobinary receiver," *IEEE Photon. Technol. Lett.*, vol. 6, pp. 648–650, May 1994.
[2] X. Gu and L. C. Blank, "10 Gbit/s unrepeatered three-level optical transmission over 100 km of standard fiber," *Electron. Lett.*, vol. 29, no. 25, pp. 2209–2211, 1993.
[3] X. Gu *et al.*, "10 Gbit/s, 138 km uncompensated duobinary transmission over installed standard fiber," *Electron. Lett.*, vol. 30, no. 23, pp. 1953–1954, 1994.
[4] K. Yonenaga *et al.*, "Optical duobinary transmission system with no receiver sensitivity degradation," *Electron. Lett.*, vol. 31, no. 4, pp. 302–304, 1995.

A. Soto and W. Soto
Authorized licensed use limited to: University of Nevada Las Vegas. Downloaded on June 10,2023 at 20:47:21 UTC from IEEE Xplore. Restrictions apply. IPR2023-00838
Exhibit 2002
Page 13

[5] A. J. Price and N. Le Mercier, "Reduced bandwidth optical digital intensity modulation with improved chromatic dispersion tolerance," *Electron. Lett.*, vol. 31, no. 1, pp. 58–59, 1995.
[6] S. Kuwano *et al.*, "10 Gbit/s repeaterless transmission experiment of optical duobinary modulated signal," *Electron. Lett.*, vol. 31, no. 16, pp. 1359–1361, 1995.
[7] A. J. Price *et al.*, "210 km repeaterless 10 Gb/s transmission experiment through nondispersion-shifted fiber using partial response scheme," *IEEE Photon. Technol. Lett.*, vol. 7, pp. 1219–1221, Oct. 1995.
[8] Y. Yano *et al.*, "2.6 Terabit/s WDM transmission experiment using optical duobinary coding," in *Proc. ECOC'96*, vol. 5, (post-deadline paper ThB.3.1), Sept. 1996.
[9] T. Ito *et al.*, "Feasibility study on over 1 bit/s/Hz high spectral efficiency WDM with optical duobinary coding and polarization interleave multiplexing," in *Proc. OFC'97*, 1997, vol. TuJ1, pp. 43–45.
[10] S. Walklin and J. Conradi, "A 10 Gb/s 4-ary ASK lightwave system," in *Proc. IOOC-ECOC97*, Edinburg, Scotland, Sept. 1997.
[11] B. Wedding *et al.*, "Multi-level dispersion supported transmission at 20 gbit/s over 46 km installed standard singlemode fiber," in *Proc. ECOC'96*, Sept. 1996, paper MoB.4.4, pp. 91–94.
[12] A. Lender, "Correlative digital communication techniques," *IEEE Trans. Commun. Technol.*, vol. COM-12, pp. 128–135, 1964.
[13] ——, "Correlative level coding for binary-data transmission," *IEEE Spectrum*, 1966, pp. 104–115.
[14] K. Feher and A. Lender, *Digital Communications, Microwave Applications.* Englewood Cliffs, NJ: Prentice Hall, 1981, pp. 144–182.
[15] S. Walklin and J. Conradi, "Effect of Mach-Zehnder modulator DC extinction ratio on residual chirp-induced dispersion in 10 Gb/s binary and AM-PSK duobinary lightwave systems," *IEEE Photon. Technol. Lett.*, vol. 9, pp. 1400–1402, Oct. 1997.
[16] J. C. Cartledge and A. F. Elrefaie, "Effect of chirping-induced waveform distortion on the performance of direct detection receivers using traveling-wave semiconductor optical preamplifiers," *J. Lightwave Technol.*, vol. 9, pp. 209–219, Feb. 1991.
[17] N. A. Olsson "Lightwave systems with optical amplifiers," *J. Lightwave Technol.*, vol. 7, pp. 1071–1082, July 1989.
[18] S. Yamamoto *et al.*, "Analysis of laser phase noise to intensity noise conversion by chromatic dispersion in intensity modulation and direct detection optical-fiber transmission," *J. Lightwave Technol.*, vol. 8, pp. 1716–1722, Nov. 1990.
[19] K. Petermann, "FM-AM noise conversion in dispersive single-mode fiber transmission lines," *Electron. Lett.*, vol. 26, no. 25, pp. 2097–2098, Dec. 1990.
[20] S. Walklin and J. Conradi, "On the relationship between chromatic dispersion and transmitter filter response in duobinary optical communication systems," *IEEE Photon. Technol. Lett.*, vol. 9, pp. 1005–1007, July 1997. (See also comments on and author's response to comment on this paper, *IEEE Photon. Technol. Lett.*, vol. 10, pp. 902–903, June 1998.)
[21] A. H. Gnauck *et al.*, "Dispersion penalty reduction using an optical modulator with adjustable chirp," *IEEE Photon. Technol. Lett.*, vol. 3, pp. 916–918, Oct. 1991.
[22] J. C. Cartledge and R. G. Mckay, "Performance of 10 Gb/s lightwave systems using an adjustable chirp optical modulator and linear equalization," *IEEE Photon. Technol. Lett.*, vol. 4, pp. 1394–1397, Dec. 1992.
[23] D. Penninckx, "Effect of electrical filtering of duobinary signals on the chromatic dispersion transmission limitations," in *Proc. ECOC'98*, Oct. 1998.
[24] S. Walklin, "Multilevel signaling for increasing the capacity of high-speed optical communication systems," Ph.D. dissertation, Univ. Alberta, Canada, Fall 1997.

Sheldon Walklin (M'97), photograph and biography not available at the time of publication.

Jan Conradi (SM'83), photograph and biography not available at the time of publication.

Authorized licensed use limited to: University of Nevada Las Vegas. Downloaded on June 10,2023 at 20:47:21 UTC from IEEE Xplore. Restrictions apply.
A. Soto and W. Soto
IPR2023-00838
Exhibit 2002
Page 14